LA-5132-MS

Nonlinear Diffusion of Pulsed Magnetic Fields in Planar and Cylindrical Plasmas

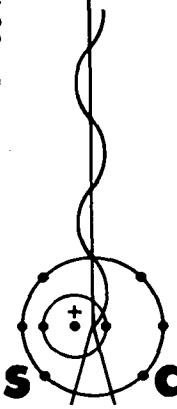

los alamos
scientific laboratory
of the University of California
LOS ALAMOS, NEW MEXICO 87544

UNITED STATES
ATOMIC ENERGY COMMISSION
CONTRACT W-7405-ENG. 36

Printed in the United States of America. Available from
National Technical Information Service
U. S. Department of Commerce
5285 Port Royal Road
Springfield, Virginia 22151
Price: Printed Copy $3.00; Microfiche $0.95

LA-5132-MS
UC-20
ISSUED: June 1973

los alamos
scientific laboratory
of the University of California
LOS ALAMOS, NEW MEXICO 87544

Nonlinear Diffusion of Pulsed Magnetic Fields in Planar and Cylindrical Plasmas

by

Albert Haberstich

NONLINEAR DIFFUSION OF PULSED MAGNETIC FIELDS IN PLANAR AND CYLINDRICAL PLASMAS

by

Albert Haberstich

ABSTRACT

The one-dimensional, one-component, nonlinear diffusion of pulsed magnetic fields in planar and cylindrical geometries is examined. The diffusion coefficient μ depends abruptly on the current density j associated with the gradient of the magnetic field. The coefficient μ is large when $j \geq j_1$, small when $j \leq j_2$, and depends linearly on j in the interval $j_2 < j < j_1$, where j_1 and j_2 are given current densities. A traveling wave solution is obtained in planar geometry and it is found that the product μj remains continuous in space in the limit $(j_1 - j_2) \to 0$. Analytic and finite difference solutions of the traveling wave problem are compared, numerical stability conditions are found, and an estimate of the numerical error is obtained. The pulsed magnetic field problem is then solved numerically in the two geometries. Large portions of the magnetic field profiles exhibit a nearly uniform current density distribution at some time during the diffusion.

I. INTRODUCTION

Plasmas are compressed and heated in theta and Z pinches by a fast rising external magnetic field. This magnetic field is produced by an external coil in the theta pinch and by a current running through the discharge in the Z pinch.

Due to the finite electrical resistivity of the pinch, the pulsed magnetic field gradually diffuses into the plasma. The rate of diffusion was measured in both configurations and was found to be more rapid than expected from classical electrical resistivity.[1-4] The diffusion is enhanced during the early stage of the pinch when the current density induced by the magnetic field gradient is concentrated in a narrow discharge region. The anomalously large resistivity appears to be due to a microinstability that is excited when the absolute value j of the current density exceeds a certain threshold j_c.[1-3]

This effect can be included in hydromagnetic calculations by allowing the electrical resistivity to become anomalous whenever the local value of j exceeds j_c.[1-5] The hydromagnetic calculation then involves solving a highly nonlinear diffusion problem. We propose to explore some of the analytical and numerical properties of this diffusion problem.

We write the diffusion equation in a one-component, one-dimensional form and assume that the diffusion coefficient μ, associated with the electrical resistivity of the plasma, is of the form shown in Fig. 1. The problem then becomes similar to a Stefan problem.[6] The diffusion coefficient of the Stefan problem, however, would depend on B rather than on the spatial derivative of B. Therefore, the Stefan solution does not seem to be directly applicable.

Here we seek a traveling wave solution of the diffusion equation in planar geometry. We divide this solution into the three regions, where $j > j_1$, $j < j_2$, and $j_2 \leq j \leq j_1$, and find that the spatial width of the transition region $j_2 \leq j \leq j_1$ remains finite in the limit $(j_1 - j_2) \to 0$. The product μj, which is proportional to the electric field in the plasma, then remains continuous in space.

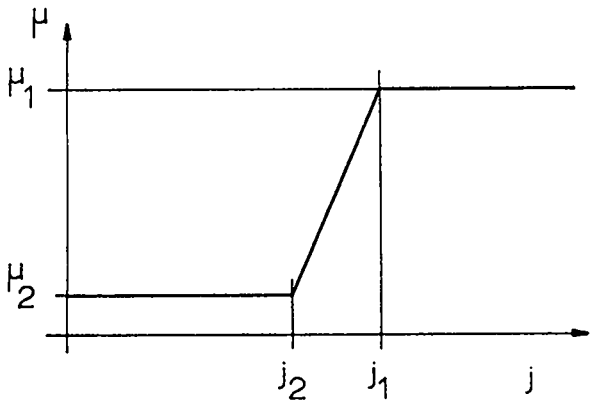

Fig. 1. Diffusion coefficient μ as a function of the absolute value of the current density j.

We also solve the problem numerically using finite difference explicit and implicit schemes. We write these schemes in such a way as to conserve magnetic fluxes. We find that, for small time and space increments, the numerical solutions can be stable and that they agree closely with the analytic traveling wave solution. It appears, therefore, that the scheme used in our earlier numerical MHD calculations[4] is adequate to handle this type of diffusion problem, at least in a planar approximation.

We make use of the explicit difference scheme to solve basic pulsed magnetic field diffusion problems in planar and cylindrical geometries, and find that large portions of the pinch may become part of the transition region, and may therefore exhibit a uniform current density distribution.

II. ANALYTIC TRAVELING WAVE SOLUTION IN PLANAR GEOMETRY

The nonlinear diffusion problem discussed above can be reduced to the one-dimensional, one-component diffusion equation

$$\frac{\partial B}{\partial t} = \frac{\partial}{\partial x}\left(\mu \frac{\partial B}{\partial x}\right) \quad , \tag{1}$$

where t is the time, x is the x-coordinate, B is the magnetic field, and μ is the diffusion coefficient of the form shown in Fig. 1.

In Fig. 1, $j = |\partial B/\partial x|$ is the absolute value of the current density. The coefficients μ_1 and μ_2 are constants, respectively proportional to the anomalous and classical resistivities of the plasma.

The transition from μ_1 to μ_2 takes place linearly over the current density interval j_1 to j_2. Thus,

$$\mu = \begin{cases} \mu_2 & , \ j < j_2 \quad , \\ \mu_c + \frac{\Delta\mu}{\Delta j}\left(j - j_c\right) & , \ j_2 \le j \le j_1 \quad , \\ \mu_1 & , \ j > j_1 \quad , \end{cases} \tag{2}$$

where

$$j_c = \tfrac{1}{2}(j_1 + j_2) \quad , \qquad \Delta j = j_1 - j_2 \quad ,$$

$$\mu_c = \tfrac{1}{2}(\mu_1 + \mu_2) \quad , \text{ and } \quad \Delta\mu = \mu_1 - \mu_2 \quad .$$

We assume that μ_1 is always larger or equal to μ_2.

Equations (1) and (2) have an analytic traveling wave solution, which is defined as a solution that travels undistorted at constant velocity v, here chosen in the positive x-direction.[7] In Fig. 2, B(x,t) then consists of a leading edge $x > x_2$ where $j < j_2$, a transition region $x_1 \le x \le x_2$ where $j_2 \le j \le j_1$, and a region $x < x_1$ where $j > j_1$. The boundaries x_1 and x_2 satisfy $x_1 = x_{10} + vt$ and $x_2 = x_{20} + vt$. Either x_{10} or x_{20} can be chosen arbitrarily.

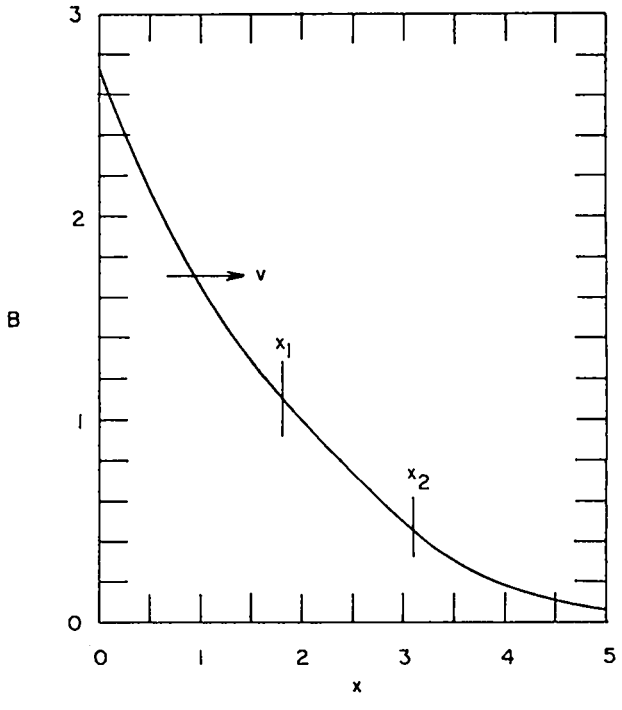

Fig. 2. Analytic traveling wave solution for v = 1, $\mu_1 = 2$, $\mu_2 = 1$, $j_c = 0.5$, and $\Delta j = 0.1$.

We solve Eqs. (1) and (2) in the three regions, match boundary conditions at x_1 and x_2, and obtain

$$B = \frac{\mu_2 j_2}{v} \exp\left(-v \frac{x - x_2}{\mu_2}\right) , \quad x > x_2 , \tag{3}$$

$$B = \frac{\mu_1 j_1}{v} \exp\left(-v \frac{x - x_1}{\mu_1}\right) , \quad x < x_1 , \tag{4}$$

and

$$x - x_1 = \frac{1}{v}\left[\left(2\mu_1 + b\right) - \left(b^2 + 4\ avB\right)^{\frac{1}{2}} + b \ln \frac{b + (b^2 + 4\ avB)^{\frac{1}{2}}}{2(\mu_1 + b)}\right] , \quad x_1 \le x \le x_2 , \tag{5}$$

where

$$a = \frac{\Delta\mu}{\Delta j} \quad \text{and} \quad b = \frac{\mu_1 j_2 - \mu_2 j_1}{\Delta j} .$$

The ratio of the magnetic fields $B(x_1) = B_1$ and $B(x_2) = B_2$ at the boundaries of the transition region follows from Eqs. (3) and (4),

$$\frac{B_1}{B_2} = \frac{\mu_1 j_1}{\mu_2 j_2} .$$

Taking the spatial derivative of Eqs. (3) through (5), we obtain the absolute current densities

$$j = j_2 \exp\left(-v \frac{x - x_2}{\mu_2}\right) , \quad x > x_2 , \tag{6}$$

$$j = j_1 \exp\left(-v \frac{x - x_1}{\mu_1}\right) , \quad x < x_1 , \tag{7}$$

and

$$x - x_1 = \frac{1}{v}\left[2a(j_1 - j) + b \ln \frac{j}{j_1}\right] , \quad x_1 \le x \le x_2 . \tag{8}$$

The width $(x_2 - x_1)$ of the transition region is a special case of Eq. (8),

$$x_2 - x_1 = \frac{1}{v}\left(2\Delta\mu + b \ln \frac{j_2}{j_1}\right) . \tag{9}$$

It is of interest to note that[8]

$$\lim_{\Delta j \to 0}(x_2 - x_1) = \frac{\Delta\mu}{v} . \tag{10}$$

Thus, the transition region width remains finite in the limit $\Delta j \to 0$. Letting $\Delta j \to 0$ in Eq. (8), we find that j becomes a linear function of x in the transition region and that the product μj, which is proportional to the electric field in the plasma, remains continuous throughout x-space.

III. NUMERICAL TRAVELING WAVE SOLUTION IN PLANAR GEOMETRY

Equations (1) and (2) are solved with the following magnetic flux conserving explicit and implicit difference schemes[9]

$$B^{n+1}_{i+\frac{1}{2}} - B^{n}_{i+\frac{1}{2}} = \frac{\Delta t}{(\Delta x)^2}\left[\left(B^{n}_{i+3/2} - B^{n}_{i+\frac{1}{2}}\right)\mu^{n}_{i+1} - \left(B^{n}_{i+\frac{1}{2}} - B^{n}_{i-\frac{1}{2}}\right)\mu^{n}_{i}\right] \tag{11}$$

and

$$B^{n+1}_{i+\frac{1}{2}} - B^{n}_{i+\frac{1}{2}} = \frac{\Delta t}{(\Delta x)^2}\left[\left(B^{n+1}_{i+3/2} - B^{n+1}_{i+\frac{1}{2}}\right)\mu^{n+1}_{i+1} - \left(B^{n+1}_{i+\frac{1}{2}} - B^{n+1}_{i-\frac{1}{2}}\right)\mu^{n+1}_{i}\right] , \tag{12}$$

respectively, where $t = n\,\Delta t$ and $x = i\,\Delta x$. The diffusion coefficients μ^{n}_{i} and μ^{n+1}_{i} are given by

$$\mu^{n,n+1}_{i} = \begin{cases} \mu_2 , & j^{n,n+1}_{i} < j_2 , \\ \mu_c + \dfrac{\Delta\mu}{\Delta j}\left(j^{n,n+1}_{i} - j_c\right) , & j_2 \le j^{n,n+1}_{i} \le j_1 , \\ \mu_1 , & j^{n,n+1}_{i} > j_1 , \end{cases} \tag{13}$$

and

$$j^{n,n+1}_{i} = \frac{1}{\Delta x}\left(B^{n,n+1}_{i-\frac{1}{2}} - B^{n,n+1}_{i+\frac{1}{2}}\right) . \tag{14}$$

In the regions of uniform μ, Eq. (11) is subject to the numerical stability condition

$$\frac{\Delta t}{(\Delta x)^2}\,\mu \le 1/2 \,, \tag{15}$$

whereas Eq. (12) is always stable.[9] The numerical stability of the explicit scheme in the transition region is derived in Appendix A and is given by

$$\frac{\Delta t}{(\Delta x)^2}\,\mu_c \le \tfrac{1}{2}\,\frac{1}{1+\frac{\Delta\mu}{\mu_c}\left(1+\frac{j_c}{\Delta j}\right)} \,. \tag{16}$$

The advanced diffusion coefficient in the transition region is not known *a priori*. We therefore determine μ_i^{n+1} by the iterative procedure

$$\mu_i^{n+1,m+1} = (1-A)\,\mu_i^{n+1,m} + A\,\bar{\mu}_i^{n+1,m} \,, \tag{17}$$

where $0 < A \le 1$ is a relaxation factor. The diffusion coefficient $\mu_i^{n+1,m+1}$ is used in the new iteration, $\mu_i^{n+1,m}$ is the coefficient used during the mth iteration, and $\bar{\mu}_i^{n+1,m}$ is calculated by Eqs. (13) and (14), using the magnetic fields obtained by the mth iteration. This procedure is repeated until $\bar{\mu}_i^{n+1,m+1}$ approaches $\mu_i^{n+1,m+1}$ to within a certain accuracy. The stability of the implicit scheme then depends on the convergence of the iteration scheme. The stability condition, derived in Appendix B, is

$$\frac{\Delta t}{(\Delta x)^2}\,\mu_c \le \tfrac{1}{4}\,\frac{\frac{2}{A}-1}{\frac{\Delta\mu}{\mu_c}\left[\left(\frac{1}{A}-1\right)+\frac{j_c}{\Delta j}\right]-\left(\frac{2}{A}-1\right)} \,. \tag{18}$$

The accuracy of the two numerical schemes can be determined by comparing numerical solutions of the traveling wave problem with the analytic solution. The numerical error in the uniform μ regions can be predicted. We define the relative error ϵ as

$$\epsilon = \left(B_{\text{numerical}} - B_{\text{analytic}}\right) \Big/ B_{\text{analytic}} \,,$$

and find it to the lowest order in Δx and Δt,

$$\epsilon = \left[\frac{1}{12}\frac{v^4}{\mu^3}\,(\Delta x)^2 \mp \frac{1}{2}\frac{v^4}{\mu^2}\,\Delta t\right] t \,, \tag{19}$$

where the upper and lower signs apply to the explicit and implicit schemes, respectively. This numerical error can be eliminated by adding a small correction $\delta\mu$ to the diffusion coefficient. For small values of Δx and Δt we find that

$$\delta\mu = \frac{\mu}{2}\,\frac{-\nu-\frac{1}{6}}{\left(\frac{\mu}{v\,\Delta x}\right)^2+\nu+\frac{1}{12}} \,, \tag{20}$$

for the implicit scheme, and that

$$\delta\mu = \frac{\mu}{2}\,\frac{\nu-\frac{1}{6}}{\left(\frac{\mu}{v\,\Delta x}\right)^2+\frac{1}{12}} \tag{21}$$

for the explicit scheme, where $\nu = \mu\,\Delta t/(\Delta x)^2$.

The accuracy of the numerical schemes in the transition region is determined experimentally. Starting at $t = 0$, with the initial state prescribed by Eqs. (3) through (5), we numerically advance the traveling wave solution shown earlier in Fig. 2. The values of B at the boundaries $x = 0$ and $x = 5$ are varied at the rates predicted by Eqs. (3) and (4). Here we add the small correction $\delta\mu$ to the diffusion coefficient to allow for the error anticipated in the regions of constant μ, and thus delay the effect of the boundaries $x = 0$ and $x = 5$ on the numerical error in the transition region.

A typical observed error ϵ is shown in Fig. 3 as a function of x at four consecutive times in the diffusion. The shape of $\epsilon(x)$ varies as the transition region traverses the mesh structure. A plot of the peak absolute error $|\hat{\epsilon}|$ as a function of time is shown in Fig. 4, whereas $\langle|\epsilon|\rangle$, the absolute value of ϵ averaged over the interval $0 \le x \le 5$ as a function of time, is shown in Fig. 5. Figures 4 and 5 were obtained with the implicit scheme with $\Delta x = 0.033$. Similar calculations have been performed with $\Delta x = 0.05$ and the two calculations have been repeated with the explicit scheme.

The peak value of $|\hat{\epsilon}|$ at time nearest $t = 0.1$ is plotted in Fig. 6 as a function of Δt for the implicit scheme for the two values of Δx. The peak error is essentially independent of Δt. For small values of Δt, $|\hat{\epsilon}|$ is proportional to $(\Delta x)^2$. Mean values of $\langle|\epsilon|\rangle$ at time $t = 0.1$ are plotted in Figs. 7 and 8 as functions of Δt for $\Delta x = 0.05$. Figure 7

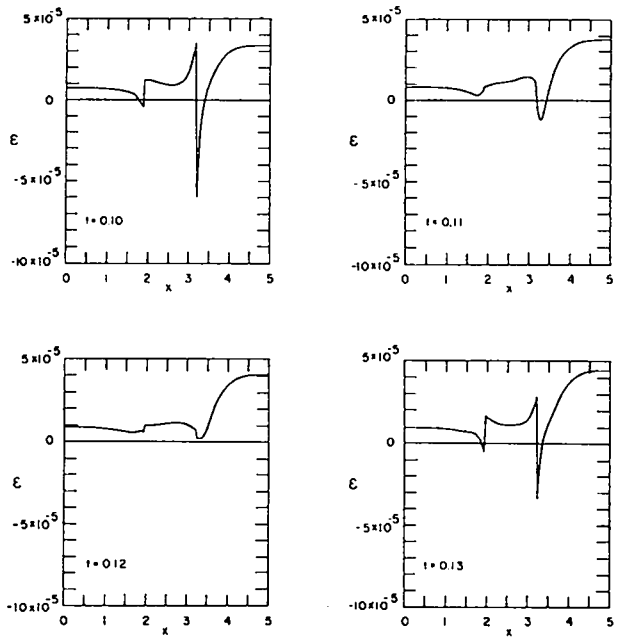

Fig. 3. Observed numerical error ε at times $t = 0.1, 0.11, 0.12$, and 0.13 of the traveling wave solution, Fig. 2, for $\Delta x = 0.033$ and $\Delta t = 5 \times 10^{-4}$. Implicit scheme.

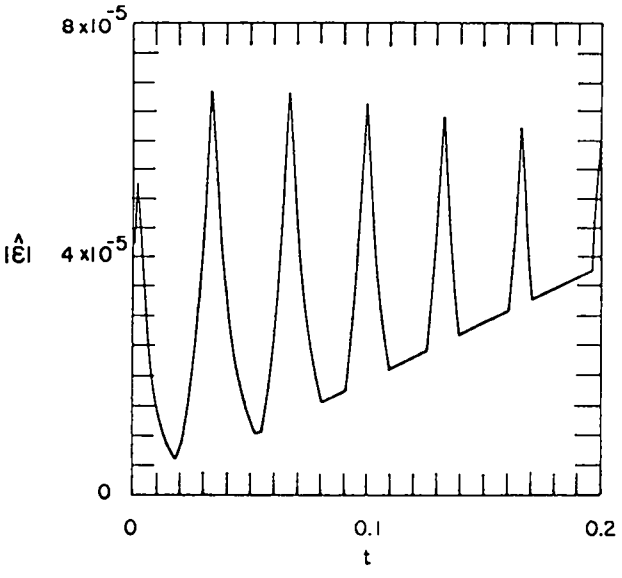

Fig. 4. Peak error $|\hat{\varepsilon}|$ as a function of time for the conditions of Fig. 2 for $\Delta x = 0.033$ and $\Delta t = 2 \times 10^{-4}$. Implicit scheme.

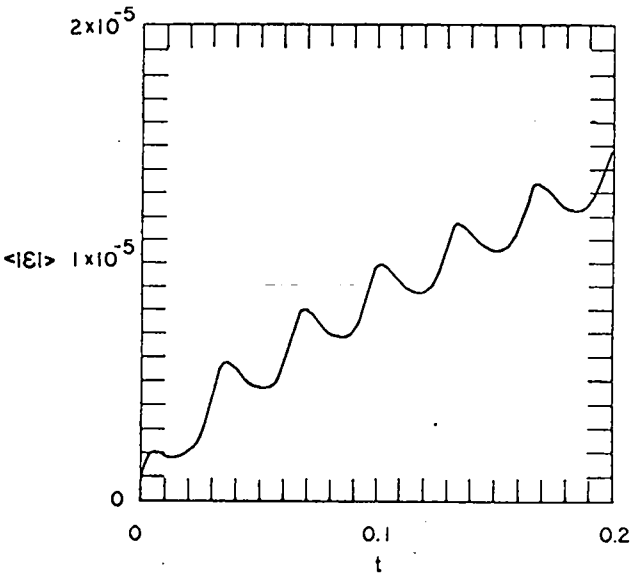

Fig. 5. Mean error $\langle|\varepsilon|\rangle$ over the interval $0 \leq x \leq 5$ as a function of time for the conditions of Fig. 2 for $\Delta x = 0.033$ and $\Delta t = 2 \times 10^{-4}$. Implicit scheme.

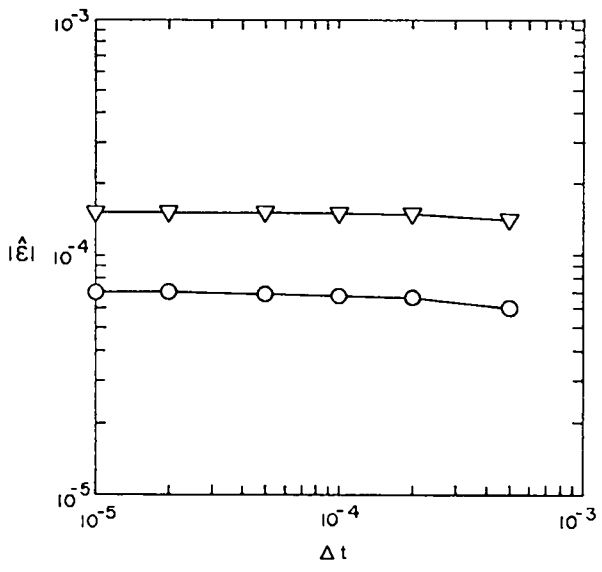

Fig. 6. Peak value of $|\hat{\varepsilon}|$ at time nearest $t = 0.1$ as a function of Δt for the conditions of Fig. 2 with $\Delta x = 0.05$ (triangles) and $\Delta x = 0.033$ (circles). Implicit scheme.

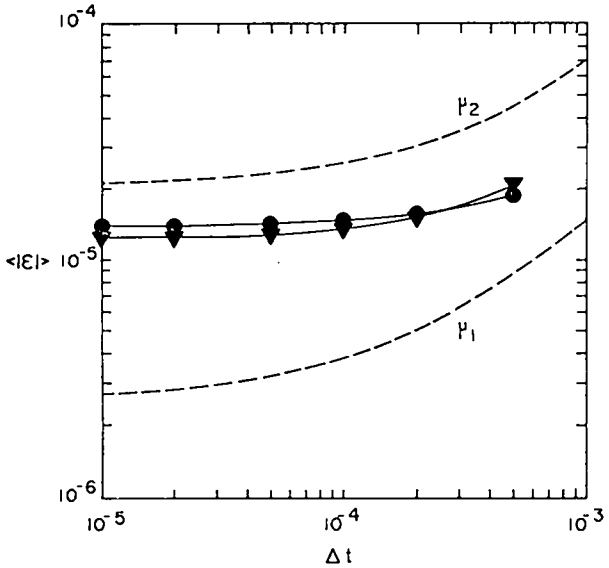

Fig. 7. Mean error $\langle|\varepsilon|\rangle$ at time t = 0.1 as a function of Δt for the conditions of Fig. 2 and $\Delta x = 0.05$. $|\varepsilon|$ averaged over the interval $0 \leq x \leq 5$ (triangles) and over the transition region only (circles). Implicit scheme.

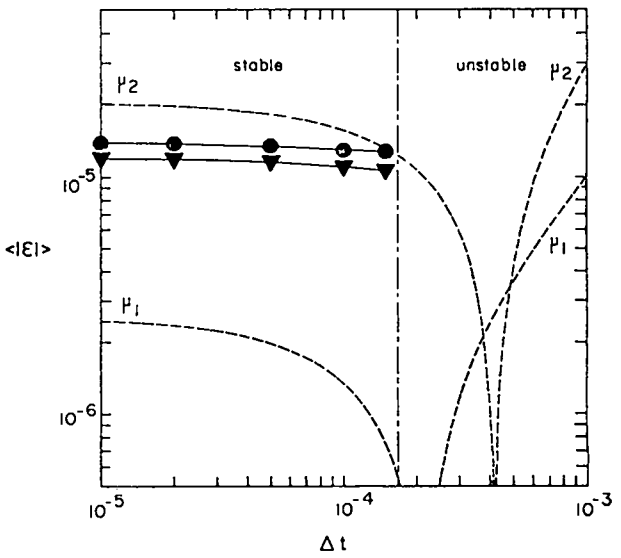

Fig. 8. Same as Fig. 7, but explicit scheme.

corresponds to the implicit scheme and Fig. 8 to the explicit solution. The triangles indicate averages over the interval $0 \leq x \leq 5$, whereas the circles correspond to averages over the transition region only. The dashed lines obtained from Eq. (19) show the error associated with the regions of uniform μ_1 and μ_2. The $\Delta x = 0.033$ calculation indicates that for small values of Δt, $\langle|\varepsilon|\rangle$ is proportional to $(\Delta x)^2$ as in the uniform μ case. For large Δt, $\langle|\varepsilon|\rangle$ increases with Δt in the implicit case. The large Δt region is not accessible to the explicit scheme.

The results obtained in this section indicate that the explicit and implicit schemes can be stable and that the numerical errors can be made negligibly small by choosing a small Δx, which in turn calls for a small value of Δt to satisfy stability requirements.

IV. DIFFUSION OF PULSED MAGNETIC FIELD IN PLANAR GEOMETRY

Having established the stability and accuracy of Eqs. (11) and (12), we can use these schemes to calculate the diffusion of pulsed magnetic fields into a semi-infinite plasma. The plasma is uniform and extends over the region x = 0 to infinity. The magnetic field is uniform in the region x = 0 to minus infinity and is pulsed from zero to $B = B_o$ at time t = 0. Thus, in addition to Eqs. (1) and (2), we must satisfy the initial and boundary conditions.

$$B = \begin{cases} 0 \quad , & x > 0 \quad , \quad t < 0 \quad , \\ B_o \quad , & x = 0 \quad , \quad t \geq 0 \quad . \end{cases} \tag{22}$$

Figure 9 shows an explicit solution obtained with $j_c = 0.5$, $\Delta j = 0.01$, $\mu_1 = 2$, and $\mu_2 = 0.02$. The magnetic field satisfies Eq. (22) at x = 0, whereas B = 0 at x = 5. A transition region is seen to develop. Due to the small value of Δj, B(x) is nearly linear in the transition region. The speed at which the transition region propagates can be predicted as a function of its width. In the limit $\mu_2 \to 0$

$$\frac{dx_2}{dt} = \frac{\mu_1}{x_2 - x_1} \quad . \tag{23}$$

For a semi-infinite plasma, this expression remains valid as long as the transition region does not extend to the origin x = 0.

V. DIFFUSION OF PULSED MAGNETIC FIELDS IN CYLINDRICAL GEOMETRY

The plasma here is cylindrical, axially and azimuthally symmetric, and has the radius r_a. The magnetic field can have two components, B_z and B_θ. We consider the two cases separately.

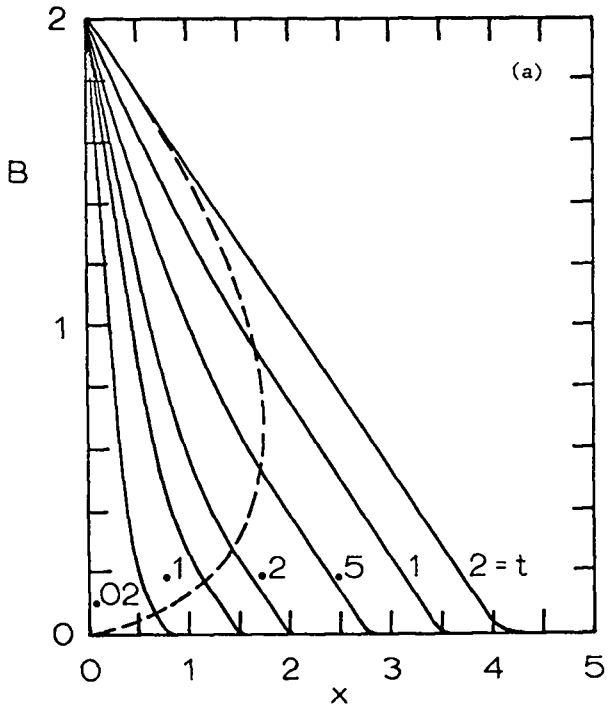

(a) B(x) as a function of time. The dashed line shows the trajectory of $B(x_1)$; $B(x_2)$ is close to the abscissa.

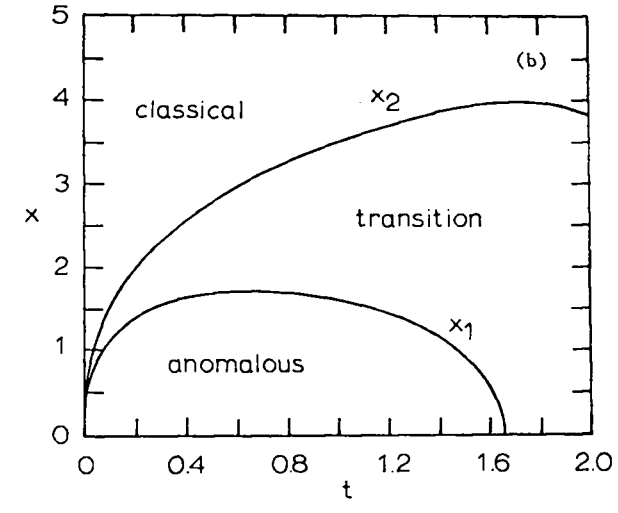

(b) x_1 and x_2 as functions of time.

Fig. 9. Diffusion of pulsed magnetic field in planar geometry. $B_o = 2$, $\mu_1 = 2$, $\mu_2 = 0.02$, $j_c = 0.5$, and $\Delta j = 0.01$.

The B_z field case is typical of a theta pinch. B_z is uniform in the outer region $r > r_a$ and is pulsed from zero to $B_z = B_{zo}$ at time $t = 0$. The initial and boundary conditions are

$$B_z = \begin{cases} 0 & , \quad r < r_a \quad , \quad t < 0 \quad , \\ B_{zo} & , \quad r = r_a \quad , \quad t \geq 0 \quad . \end{cases} \tag{24}$$

The diffusion equation in cylindrical coordinates becomes

$$\frac{\partial B_z}{\partial t} = \frac{1}{r} \frac{\partial}{\partial r} \left(\mu r \frac{\partial B_z}{\partial r} \right) \quad , \tag{25}$$

where μ is now defined in terms of $j = |j_\theta|$, with

$$j_\theta = - \frac{\partial B_z}{\partial r} \quad ,$$

and $j_\theta = 0$ on axis.

Equation (25) can be solved by finite difference schemes similar to Eqs. (11) and (12). Although the accuracy of these schemes has not been checked in cylindrical geometry, it is believed to be comparable to that of the linear schemes. It might be necessary, however, to study this point further.

The explicit difference scheme in cylindrical coordinates can be written as

$$B^{n+1}_{z,i+\frac{1}{2}} - B^{n}_{z,i+\frac{1}{2}} =$$

$$\frac{\Delta t}{(\Delta r)^2} \frac{1}{r_{i+\frac{1}{2}}} \left[r_{i+1} \mu^n_{i+1} \left(B^n_{z,i+3/2} - B^n_{z,i+\frac{1}{2}} \right) \right.$$

$$\left. - r_i \mu^n_i \left(B^n_{z,i+\frac{1}{2}} - B^n_{z,i-\frac{1}{2}} \right) \right] \quad , \tag{26}$$

where the B_z flux is conserved. The diffusion coefficient μ^n_i is defined in terms of Eq. (13) with

$$j^n_i = \frac{1}{\Delta r} \left(B^n_{z,i+\frac{1}{2}} - B^n_{z,i-\frac{1}{2}} \right) \quad .$$

Figures 10 and 11 show the numerical results obtained with $j_c = 0.5$, $\Delta j = 0.01$, $\mu_1 = 2$, and $\mu_2 = 0.02$. r_1 and r_2 are the outer and inner boundaries of the transition region, respectively. We call the case shown in Fig. 10 supercritical, meaning that $B_{zo} \geq r_a j_c$. The transition region here

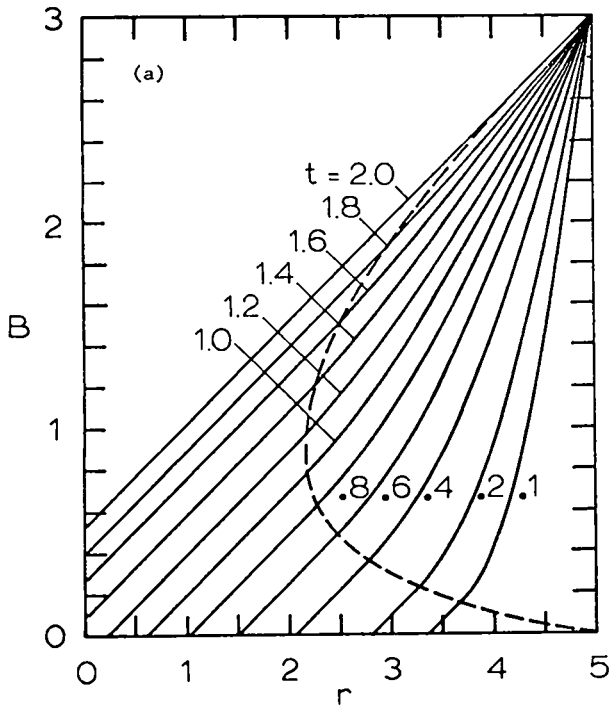

(a) $B_z(r)$ as a function of time. The dashed line represents $B_z(r_1)$; $B_z(r_2)$ is close to the abscissa.

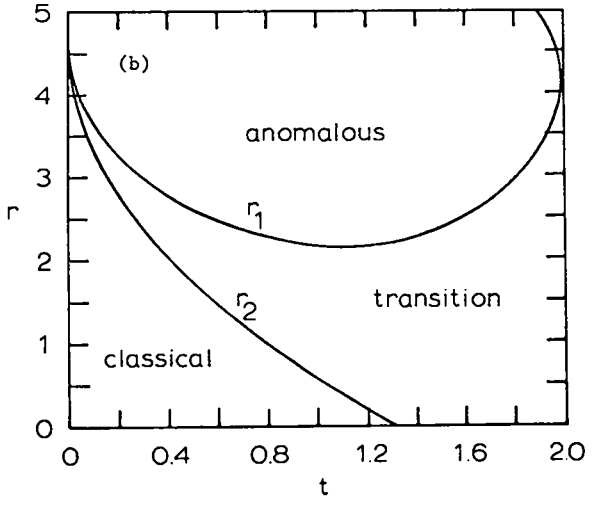

(b) r_1 and r_2 as functions of time.

Fig. 10. Diffusion of pulsed magnetic field in theta-pinch geometry with $\mu_1 = 2$, $\mu_2 = 0.02$, $j_c = 0.5$, and $\Delta j = 0.01$. $B_{zo} = 3$, supercritical.

can extend over the entire plasma radius. This situation is not possible in the subcritical case $B_{zo} < r_a j_c$ shown in Fig. 11.

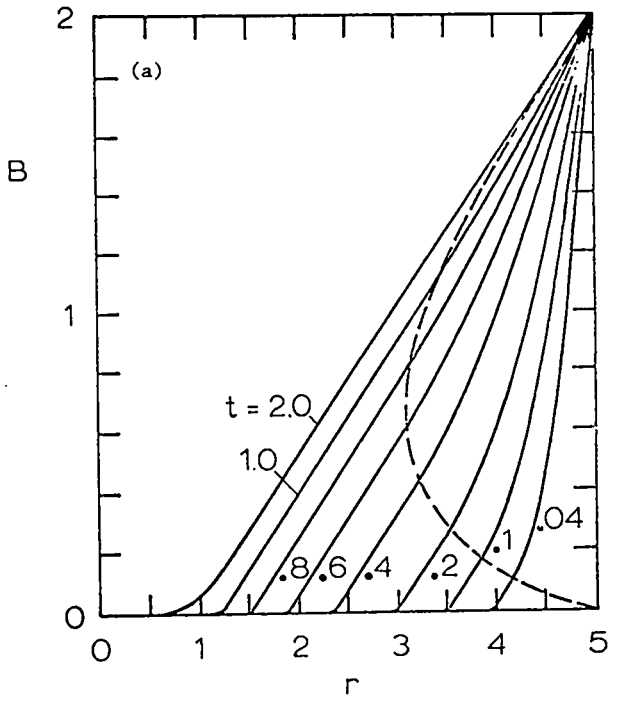

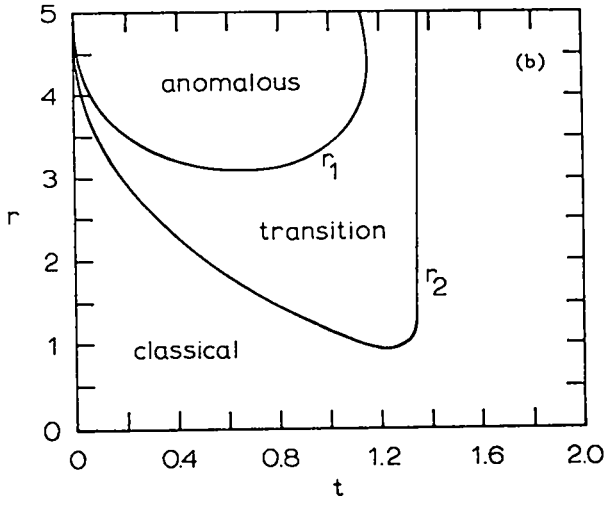

Fig. 11. Same as Fig. 10 with $B_{zo} = 2$, subcritical.

The speed of propagation of the transition region can be predicted in terms of its width $(r_1 - r_2)$ and in its position. In the limit $\mu_2 \to 0$,

$$\frac{dr_2}{dt} = - \frac{2 r_1 \mu_1}{r_1^2 - r_2^2} \quad . \tag{27}$$

This formula applies as long as the transition region does not reach the axis or the edge r_a of the plasma column.

The B_θ field case is similar to a pure Z pinch. B_θ falls as 1/r in the outer region $r > r_a$, and the field at $r = r_a$ is pulsed from zero to $B_{\theta o}$ at time $t = 0$. The initial and boundary conditions are

$$B = \begin{cases} 0 \quad , & r < r_a \quad , \quad t < 0 \quad , \\ B_{\theta o} \quad , & r = r_a \quad , \quad t \geq 0 \quad . \end{cases} \tag{28}$$

The diffusion equation becomes

$$\frac{\partial B_\theta}{\partial t} = \frac{\partial}{\partial r}\left[\frac{\mu}{r}\frac{\partial}{\partial r}\left(rB_\theta\right)\right] \quad , \tag{29}$$

where μ depends on $j = |j_z|$ and

$$j_z = \frac{1}{r}\frac{\partial}{\partial r}\left(rB_\theta\right) \quad .$$

The explicit difference scheme is written in the form

$$B^{n+1}_{\theta,i+\frac{1}{2}} - B^{n}_{\theta,i+\frac{1}{2}} = \frac{\Delta t}{(\Delta r)^2}\left[\frac{\mu^n_{i+1}}{r_{i+1}}\left(r_{i+3/2}\, B^n_{\theta,i+3/2} - r_{i+\frac{1}{2}}\, B^n_{\theta,i+\frac{1}{2}}\right) - \frac{\mu^n_i}{r_i}\left(r_{i+\frac{1}{2}}\, B^n_{\theta,i+\frac{1}{2}} - r_{i-\frac{1}{2}}\, B^n_{\theta,i-\frac{1}{2}}\right)\right] \quad , \tag{30}$$

where the B_θ flux is conserved everywhere except on the axis. The diffusion coefficient μ^n_i is defined in terms of Eq. (13) with

$$j^n_i = \frac{1}{\Delta r}\frac{1}{r_i}\left(r_{i+\frac{1}{2}}\, B^n_{\theta,i+\frac{1}{2}} - r_{i-\frac{1}{2}}\, B^n_{\theta,i-\frac{1}{2}}\right) \quad .$$

Figures 12 and 13 show numerical solutions for $j_c = 0.5$, $\Delta j = 0.01$, $\mu_1 = 2$, and $\mu_2 = 0.02$. Super- and subcritical are now defined as $B_{\theta o}$ being larger or smaller than $r_a j_c/2$, respectively. A supercritical Z pinch eventually becomes entirely anomalous, whereas a subcritical pinch becomes completely classical.

The speed of propagation of the transition region, in the limit $\mu_2 \to 0$, is given by

$$\frac{dr_2}{dt} = -\frac{\mu_1}{r_2 \ln(r_1/r_2)} \tag{31}$$

until the transition region reaches $r = 0$ or $r = r_a$.

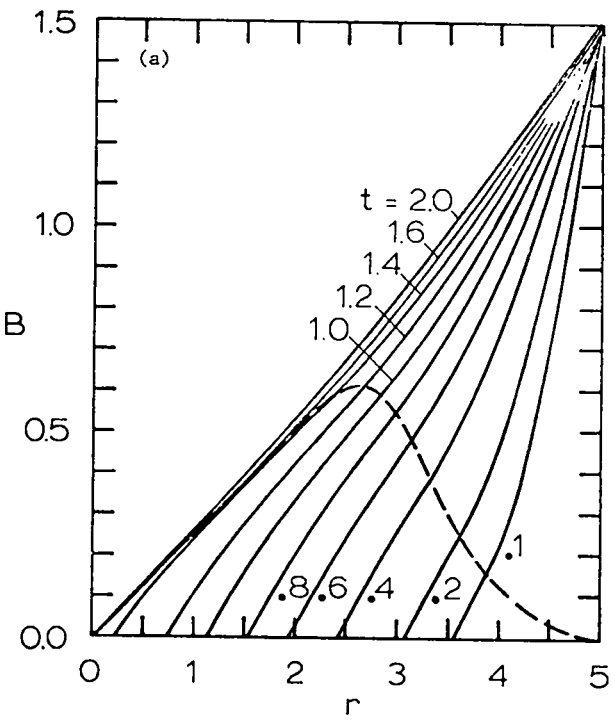

(a) $B_\theta(r)$ as a function of time. The dashed line represents $B_\theta(r_1)$; $B_\theta(r_2)$ is close to the abscissa.

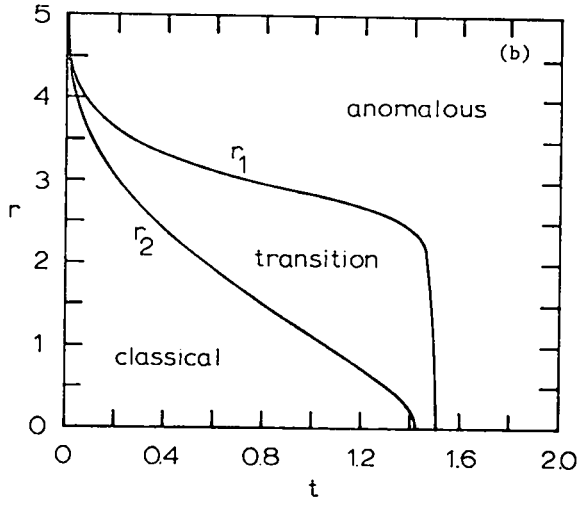

(b) r_1 and r_2 as functions of time.

Fig. 12. Diffusion of pulsed magnetic field in Z-pinch geometry with $\mu_1 = 2$, $\mu_2 = 0.02$, $j_c = 0.5$, and $\Delta j = 0.01$. $B_{\theta o} = 1.5$, supercritical.

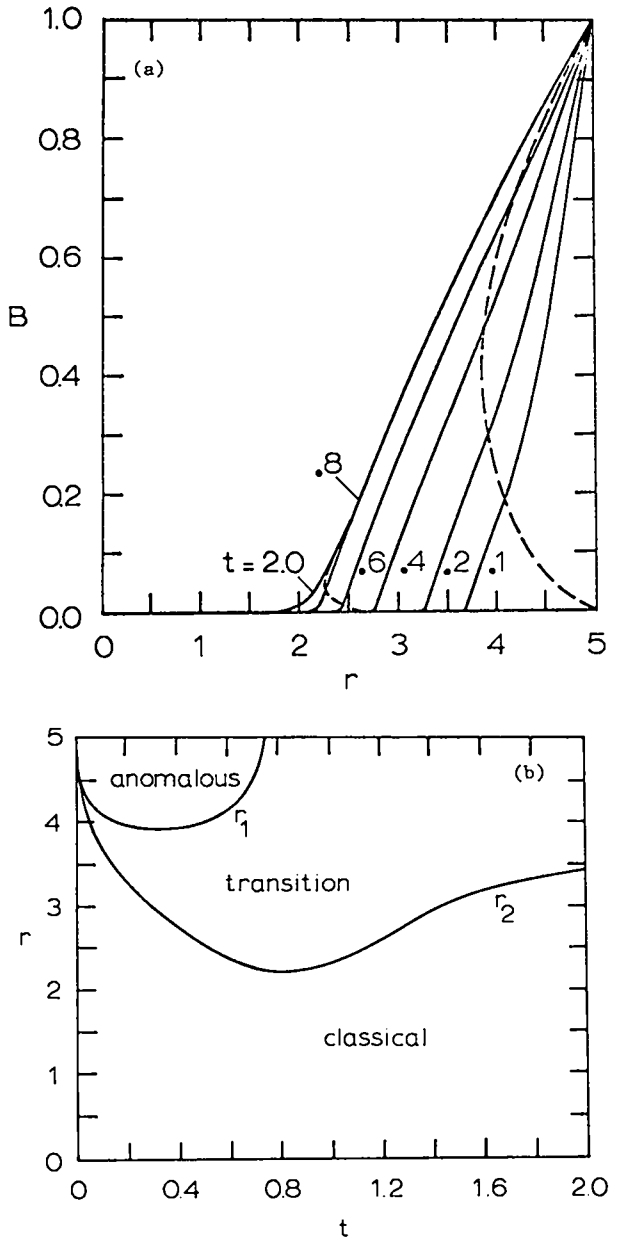

Fig. 13. Same as Fig. 12 with $B_{\theta o}$ = 1.0, subcritical.

The results obtained in this section indicate that large regions of both the theta and Z pinches can become part of the transition region. The current density can then be nearly uniform over a large portion of the discharges. This effect persists in the limit $\Delta j \to 0$. It is related to the fact that the magnetic flux must be conserved when μ_2 changes to μ_1.

ACKNOWLEDGMENTS

I wish to thank J. P. Freidberg, R. G. Kellner, M. M. Klein, J. A. Phillips, B. R. Suydam, B. K. Swartz, and H. Weitzner for their helpful discussions.

REFERENCES

1. H. A. B. Bodin, J. McCartan, A. A. Newton, and G. H. Wolf, "Diffusion and Stability of High-β Plasma in an 8-Metre Theta Pinch," in Plasma Physics and Controlled Nuclear Fusion Research (International Atomic Energy Agency, Vienna, 1969), Vol. 2, pp. 533-553.

2. H. A. B. Bodin and A. A. Newton, "Study of the Diffusion of High-β Plasma in a Theta Pinch," Phys. Fluids 12, 2175-2184 (1969).

3. H. A. B. Bodin, J. McCartan, and G. H. Wolf, "The Early Stages of a Theta Pinch," in Third European Conference on Controlled Fusion and Plasma Physics (Wolters-Noordhoff Publishing, Groningen, 1969), p. 74.

4. A. Haberstich, "Status Report of the LASL Controlled Thermonuclear Research Program for 12-Month Period Ending October 1970," Los Alamos Scientific Laboratory report LA-4585-MS (February 1971), pp. 37-39.

5. A. Haberstich, "Numerical Calculation of the Theta, Z, and Screw Pinches," Los Alamos Scientific Laboratory report LA-4782-MS (December 1971).

6. H. S. Carslaw and J. C. Jaeger, Conduction of Heat in Solids (Oxford University Press, London, 1959), pp. 282-296.

7. R. D. Richtmyer, Difference Methods for Initial-Value Problems (Interscience Publishers, Inc., New York, 1957), p. 104.

8. B. R. Suydam, Los Alamos Scientific Laboratory, personal communication, 1971.

9. R. D. Richtmyer, Difference Methods for Initial-Value Problems (Interscience Publishers, Inc., New York, 1957), p. 93, Schemes 1 and 3.

APPENDIX A

STABILITY OF THE EXPLICIT SCHEME IN THE TRANSITION REGION

We expand both B^n and B^{n+1} to the third order in Δx about a mesh center point situated in the transition region and write

$$B^n_{i+\frac{1}{2}} = a_o \quad , \qquad \text{(A-1a)}$$

$$B^n_{i-\frac{1}{2}} = a_o + a_1 \Delta x + a_2(\Delta x)^2 \quad , \qquad \text{(A-1b)}$$

$$B^n_{i+3/2} = a_o - a_1 \Delta x + a_2(\Delta x)^2 \quad , \qquad \text{(A-1c)}$$

and

$$B^{n+1}_{i+\frac{1}{2}} = b_o \quad , \qquad \text{(A-2a)}$$

$$B^{n+1}_{i-\frac{1}{2}} = b_o + b_1 \Delta x + b_2(\Delta x)^2 \quad , \qquad \text{(A-2b)}$$

$$B^{n+1}_{i+3/2} = b_o - b_1 \Delta x + b_2(\Delta x)^2 \quad . \qquad \text{(A-2c)}$$

From Eqs. (13) and (14) and Eqs. (A-1a) through (A-1c),

$$\mu^n_i = \mu_c + \frac{\Delta\mu}{\Delta j}(a_1 - j_c + a_2 \Delta x) \qquad \text{(A-3a)}$$

and

$$\mu^n_{i+1} = \mu_c + \frac{\Delta\mu}{\Delta j}(a_1 - j_c - a_2 \Delta x) \quad . \qquad \text{(A-3b)}$$

After substituting Eqs. (A-1a) through (A-3b) into the explicit difference equation, Eq. (11), we find that

$$b_o - a_o = 2\Delta t\, a_2 \left[\mu_c + \frac{\Delta\mu}{\Delta j}(2a_1 - j_c)\right]$$

To determine the stability of the explicit scheme, we add a small perturbation of wavelength $2\Delta x$ and amplitude ϵ_a to B^n.

Thus,

$$B^n_{i+\frac{1}{2}} = a_o + \epsilon_a \quad , \qquad \text{(A-5a)}$$

$$B^n_{i-\frac{1}{2}} = a_o + a_1 \Delta x + a_2(\Delta x)^2 - \epsilon_a \quad , \qquad \text{(A-5b)}$$

and

$$B^n_{i+3/2} = a_o - a_1 \Delta x + a_2(\Delta x)^2 - \epsilon_a \quad . \qquad \text{(A-5c)}$$

Then

$$\mu^n_i = \mu_c + \frac{\Delta\mu}{\Delta j}\left[a_1 - j_c + \left(a_2 \Delta x - 2\frac{\epsilon_a}{\Delta x}\right)\right] \qquad \text{(A-6a)}$$

and

$$\mu^n_{i+1} = \mu_c + \frac{\Delta\mu}{\Delta j}\left[a_1 - j_c - \left(a_2 \Delta x - 2\frac{\epsilon_a}{\Delta x}\right)\right] . \qquad \text{(A-6b)}$$

We assume that this perturbation gives rise to a similar perturbation ϵ_b in B^{n+1}, such that

$$B^{n+1}_{i+\frac{1}{2}} = b_o + \epsilon_b \quad , \qquad \text{(A-7a)}$$

$$B^{n+1}_{i-\frac{1}{2}} = b_o + b_1 \Delta x + b_2(\Delta x)^2 - \epsilon_b \quad , \qquad \text{(A-7b)}$$

and

$$B^{n+1}_{i+3/2} = b_o - b_1 \Delta x + b_2(\Delta x)^2 - \epsilon_b \quad . \qquad \text{(A-7c)}$$

Substituting Eqs. (A-5a) through (A-7c) into the difference equation, Eq. (11), we obtain

$$(b_o - a_o) + (\epsilon_b - \epsilon_a) = 2\Delta t\left[a_2 - 2\frac{\epsilon_a}{(\Delta x)^2}\right]\left[\mu_c + \frac{\Delta\mu}{\Delta j}(2a_1 - j_c)\right] . \qquad \text{(A-8)}$$

We now subtract the unperturbed Eq. (A-4) from Eq. (A-8), solve for ϵ_b, and find

$$\epsilon_b = \gamma\, \epsilon_a \quad , \tag{A-9}$$

where

$$\gamma = 1 - 4\,\frac{\Delta t}{(\Delta x)^2}\left[\mu_c + \frac{\Delta\mu}{\Delta j}\,(2a_1 - j_c)\right] \tag{A-10}$$

For stability, γ must satisfy $|\gamma| \leq 1$, that is,

$$4\,\frac{\Delta t}{(\Delta x)^2}\left[\mu_c + \frac{\Delta\mu}{\Delta j}\,(2a_1 - j_c)\right] \leq 2 \ . \tag{A-11}$$

The worst condition occurs for $a_1 = j_c + \Delta j/2$. The stability condition then becomes

$$\frac{\Delta t}{(\Delta x)^2}\,\mu_c \leq \frac{1}{1 + \frac{\Delta\mu}{\mu_c}\left(\frac{1}{2} + \frac{j_c}{\Delta j}\right)} \tag{A-12}$$

Equation (A-12) is plotted in Fig. A-1 where it is compared against stability limits observed experimentally on the computer.

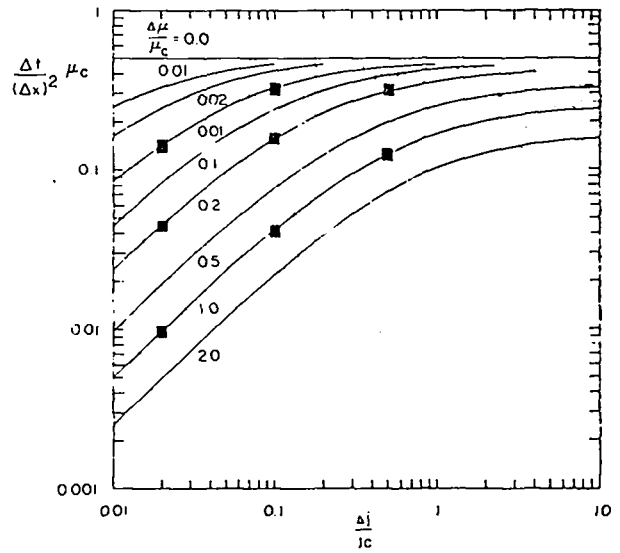

Fig. A-1. Explicit stability limits of $\mu_c \Delta t/(\Delta x)^2$ as functions of $\Delta j/j_c$ for several values of $\Delta\mu/\mu_c$. The curves are calculated from Eq. (A-12). The squares are limits observed with $x_2 - x_1 = 2.04$ and $\Delta x = 0.05$.

APPENDIX B

STABILITY OF THE IMPLICIT SCHEME IN THE TRANSITION REGION

We assume that the implicit difference equation, Eq. (12), has been solved exactly. B^{n+1} is then given by Eqs. (A-2a) through (A-2c),

$$\mu_i^{n+1} = \mu_c + \frac{\Delta\mu}{\Delta j}\,(b_1 - j_c + b_2\,\Delta x) \ , \tag{B-1a}$$

and

$$\mu_{i+1}^{n+1} = \mu_c + \frac{\Delta\mu}{\Delta j}\,(b_1 - j_c - b_2\,\Delta x) \ . \tag{B-1b}$$

Substituting Eqs. (A-1a) through (A-2c) and Eqs. (B-1a) and (B-1b) into the difference equation, Eq. (12), we find that

$$b_o - a_o = 2\,\Delta t\, b_2\left[\mu_c + \frac{\Delta\mu}{\Delta j}\,(2b_1 - j_c)\right]. \tag{B-2}$$

To determine the stability of the iteration scheme, Eq. (17), we add a small perturbation of wavelength $2\Delta x$ and amplitude ϵ_μ to the diffusion coefficient. Then

$$\mu_i^{n+1,m} = \mu_c + \frac{\Delta\mu}{\Delta j}\,(b_1 - j_c + b_2\,\Delta x) + \epsilon_\mu^m \tag{B-3a}$$

and

$$\mu_{i+1}^{n+1,m} = \mu_c + \frac{\Delta\mu}{\Delta j}\,(b_1 - j_c - b_2\,\Delta x) - \epsilon_\mu^m \ . \tag{B-3b}$$

We assume that this perturbation causes a similar perturbation of amplitude ϵ_b in B^{n+1}. Substituting Eqs. (A-1a) through (A-1c), Eqs. (A-7a) through

(A-7c), as well as Eqs. (B-3a) and (B-3b) into the implicit difference equation, Eq. (12), we find that

$$b_o - a_o + \epsilon_b^m = 2\,\Delta t \left\{ b_2 \left[\mu_c + \frac{\Delta\mu}{\Delta j}\,(2b_1 - j_c) \right] + b_1\,\frac{\epsilon_\mu^m}{\Delta x} - 2\,\frac{\epsilon_b^m}{(\Delta x)^2}\left[\mu_c + \frac{\Delta\mu}{\Delta j}\,(b_1 - j_c) \right] \right\} . \tag{B-4}$$

We subtract the unperturbed Eq. (B-2) from Eq. (B-4), solve for ϵ_b^m, and obtain

$$\epsilon_b^m = \gamma\,\epsilon_\mu^m \quad , \tag{B-5}$$

where

$$\gamma = 2\,\frac{\Delta t}{(\Delta x)^2}\,\frac{b_1\,\Delta x}{1 + 4\,\frac{\Delta t}{(\Delta x)^2}\left[\mu_c + \frac{\Delta\mu}{\Delta j}\,(b_1 - j_c) \right]} . \tag{B-6}$$

In terms of $B^{n+1,m}$,

$$\bar{\mu}_i^{n+1,m} = \mu_c + \frac{\Delta\mu}{\Delta j}\left[b_1 - j_c + \left(b_2\,\Delta x - 2\,\frac{\epsilon_b^m}{\Delta x} \right) \right] \tag{B-7a}$$

and

$$\bar{\mu}_{i+1}^{n+1,m} = \mu_c + \frac{\Delta\mu}{\Delta j}\left[b_1 - j_c - \left(b_2\,\Delta x - 2\,\frac{\epsilon_b^m}{\Delta x} \right) \right] . \tag{B-7b}$$

With these coefficients and using Eq. (17), $\mu^{n+1,m+1}$ becomes

$$\mu_i^{n+1,m+1} = \mu_c + \frac{\Delta\mu}{\Delta j}\,(b_1 - j_c + b_2\,\Delta x) + \epsilon_\mu^{m+1} \quad , \tag{B-8}$$

where

$$\epsilon_\mu^{m+1} = \epsilon_\mu^m \left[(1 - A) - 2A\,\frac{\Delta\mu}{\Delta j}\,\frac{\gamma}{\Delta x} \right] . \tag{B-9}$$

For stability, it is necessary that

$$\left| \epsilon_\mu^{m+1} \right| \le \left| \epsilon_\mu^m \right| \quad , \tag{B-10}$$

that is,

$$A\left(1 + 2\,\frac{\Delta\mu}{\Delta j}\,\frac{\gamma}{\Delta x} \right) \le 2 . \tag{B-11}$$

Substituting for γ, we obtain the stability condition

$$4\,\frac{\Delta t}{(\Delta x)^2} \le \frac{\frac{2}{A} - 1}{b_1\,\frac{\Delta\mu}{\Delta j} - \left(\frac{2}{A} - 1 \right)\left[\mu_c + \frac{\Delta\mu}{\Delta j}\,(b_1 - j_c) \right]} . \tag{B-12}$$

The right-hand side of this expression is smallest for $b_1 = j_c - \Delta j/2$. The stability condition then becomes

$$\frac{\Delta t}{(\Delta x)^2}\,\mu_c \le \tfrac{1}{4}\,\frac{\frac{2}{A} - 1}{\frac{\Delta\mu}{\mu_c}\left[\left(\frac{1}{A} - 1 \right) + \frac{j_c}{\Delta j} \right] - \left(\frac{2}{A} - 1 \right)} . \tag{B-13}$$

Equation (B-13) is plotted in Fig. B-1 for $\Delta\mu/\mu_c = 1/1.5$. It is compared against stability limits observed experimentally on the computer.

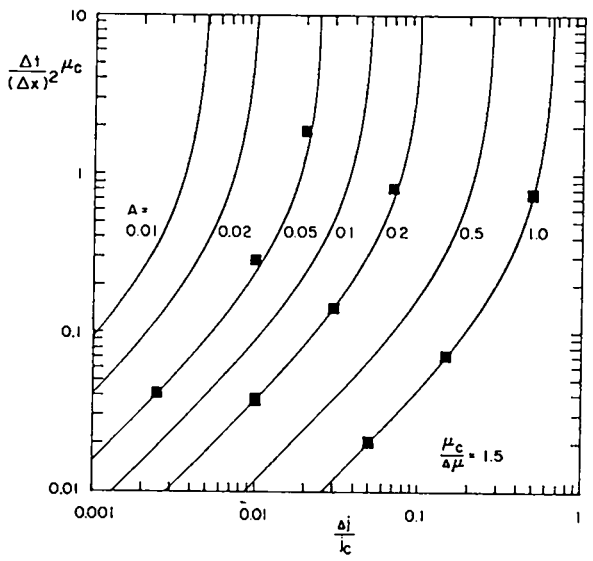

Fig. B-1. Implicit limits of $\mu_c \Delta t/(\Delta x)^2$ as functions of $\Delta j/j_c$ for several values of the relaxation factor A, with $\Delta\mu/\mu_c = 1/1.5$. The curves are calculated from Eq. (B-13). The squares are limits observed with $\mu_1 = 2$, $\mu_2 = 1$, and $\Delta x = 0.05$.

☆ U. S. GOVERNMENT PRINTING OFFICE: 1973 — 784-278/20

EE:298(60)